SIN-CHN
SCIENTIFIC PRESS PTE.LTD.

Molecular & Cellular Biomechanics 2024, 21(4), 1018.
https://doi.org/10.62617/mcb1018

Article

Biomechanical characterization of different rope skipping movements based on three-dimensional motion capture and electromyographic signal acquisition

Haoqin Li

Zhengzhou University of Industrial Technology, Zhengzhou 450064, China; 13603713805@163.com

CITATION

Li H. Biomechanical characterization of different rope skipping movements based on three-dimensional motion capture and electromyographic signal acquisition. Molecular & Cellular Biomechanics. 2024; 21(4): 1018. https://doi.org/10.62617/mcb1018

ARTICLE INFO

Received: 5 December 2024
Accepted: 18 December 2024
Available online: 30 December 2024

Abstract: Rope skipping is becoming a nationally popular sport with recreational, fitness and competitive attributes. However, poorly accomplished movements during the sport may not yield the best results and may even result in injuries. Therefore, the study used 3D motion capture and electromyographic signal acquisition for biomechanical characterization. It analyzed the human joint angles, angular velocities, muscle activation level, and muscle contribution rate in comparison when performing different rope skipping movements. The experimental results showed that the total duration of single movement was higher in the experimental group than in the control group. The average movement angle of the wrist joint in the pre-swing stage was greater for single shake than for single double shake, with the angle ranges of 116°–168° and 107°–172°, respectively. The wrist joint angular velocity of single double shake changed more gently, and the angular velocity of double shake was larger than that of single shake, with a difference of 141°. In the single-shake pre-swing stage, the activation of the trapezius and deltoid was much higher than that of the other muscles, 65% and 66%, respectively. The buffering stage contributed the most to the deltoid, with 23%, 21%, 24%, and 23% for the individual movements, respectively. As a result, the experimental group's rope skipping movements were completed more standardized, with lower free heights and better cushioning, reducing the risk of injury. The method used in the study can effectively biomechanically characterize human joints and muscles during rope skipping and improve the science and rationality of the rope skipping movement.

Keywords: three-dimensional movements; electromyographic signals; rope skipping; muscle activation level; muscle contribution rate

1. Introduction

Sports biomechanics is used to quantitatively study and analyze the mechanical state of the muscles and bodies of professional athletes in different sports, and to analyze the angles and forces of movements through mathematical models or computer simulations, etc. [1,2]. Sports biomechanics analysis can not only qualitatively analyze the mechanical characteristics, but also quantitatively analyze the magnitude of force, velocity, acceleration, etc. [3]. By analyzing these parameters, it is possible to gain a profound understanding of the movement patterns exhibited by athletes, identify the strengths and weaknesses of their sports skills in a timely manner, and implement strategies to enhance their strengths and mitigate their weaknesses [4,5]. Biomechanical analysis also plays an important role in physical education, which is mainly used to study the external mechanical movement of athletes, to help physical education teachers and students understand the mathematical model, computer simulation and measurement, and to be able to analyze the angles and forces

of sports movements [6]. This helps to accelerate the reform process of physical education and improve the quality of teaching and students' sports safety. Rope skipping is an ancient folk recreational activity and has gradually developed a variety of attributes such as fitness and competition, and at the same time, with the country's attention to sports and continuous investment [7]. The sport of rope skipping has been greatly developed in schools, and at the same time, its technical movements and competitive rules are also constantly developing and innovating. Therefore, adopting the method of sports biomechanics analysis to study the rope skipping sport makes the rope skipping more scientific and reasonable. Peng and Tang proposed a technique incorporating deep learning in order to biomechanically analyze the hitting angles of tennis players. The technique employed an IoT-based sensor image acquisition circuit to collect the athlete image data, and used a generic adversarial network with feature mapping optimization to optimize the images and analyze the joint motion metrics at different hitting angles. Experiments revealed that the technique measured knee motion speeds of 2.59 m/s and 2.21 m/s at two strike angles [8]. Tian, to study the technical characteristics of rope skipping, to improve the training efficiency as well as to reduce the risk of injury, 10 students were tested and the biomechanical characteristics during rope skipping were analyzed. The experiments showed that the range of angular changes of the lower limb joints in triple-swing rope skipping was larger than that of single-swing rope skipping in the ground-thrust phase and the hanging phase, and smaller than that of single-swing rope skipping in the buffering phase. To ensure the success of triple-swing rope skipping, the lower limbs need to exert a larger force on the ground [9]. Li et al. [10] to compare the biomechanical differences of the lower limbs during alternate rope skipping with shoes off and shoes on, the Qualisys motion capture system and Kistler force platform were used to collect joint force data and trajectories in the two cases, which were examined using the paired t-test. The experiments showed that wearing shoes resulted in a significant decrease in peak joint angular velocity at the landing node, and that wearing shoes could provide higher counterthrust by increasing the plantarflexor joint force.

Trasolini et al. [11] found that throwing sports are a common source of musculoskeletal losses in order to improve and prevent these injuries. The study analyzed the biomechanics of throwing athletes using marker-based 3D video for motion capture, using shoulder and elbow torque, shoulder rotation, kinetic chain function, and lower extremity mechanics as test metrics. Experiments indicated that this method could effectively accomplish the analysis of athlete-related data and reduce muscle damage [11]. Irawan and Prastiwi [12] biomechanically analyzed the three-point movement of basketball players in order to understand the effectiveness of the movement and improve the performance of the athletes. The study was conducted using purposive sampling calculations on ten male athletes and the movement videos were analyzed using Kinovea version 0.9.4 to obtain the corresponding movement tables. It was demonstrated that the best three-point shot was thrown with an average shoulder angle of 135.39° in the throwing phase and 134.83° in the follow-through phase [12]. Li et al. [13] proposed a biomechanical analysis method based on video images and convolutional neural networks in order to investigate the effects of stroke intensity and angle on the outcome of tennis strokes. The method extracted the athlete's ankle angle and foot displacement data during interception for analysis. The

experiments showed that the best results were obtained at the interception with the left ankle angle (103°–108°) and the right ankle angle (98°–103°), and the speed of the stroke was basically the same as the speed of the left knee [13]. Gupta et al. [14] proposed a portable electromyographic signal acquisition module in order to obtain high quality electromyographic data. The study was conducted in a controlled environment for instrument comparison and the test results were calculated for 10 subjects. The total uncertainty of the system ranged from 0.0106%–0.0196% of the root mean square (RMS). The RMS uncertainty of the existing commercial system was 0.0171%–0.0359% and the system possessed good performance and low cost [14].

To summarize, existing studies have explored the results of biomechanical analysis on different sports from various aspects, and some research results have been achieved. However, fewer studies have been conducted to analyze the rope skipping movement aspect, and their biomechanical characterization is not comprehensive. Therefore, the study proposes a biomechanical analysis of rope skipping movement based on 3D movements capture and electromyographic signal acquisition. The study innovatively employs the OpenSim model to analyze the 3D movements data of the testers, and selects people with different training levels as experimental and control groups to analyze their joint and muscle characteristics at various stages. The purpose of this study is to investigate the reasonable rope skipping movement and to provide more scientific and reasonable guidance for coaches and athletes. The study is divided into three parts. The first part describes the object of the study, the relevant instruments used in the experiment, the research methodology and the relevant steps. The second part of the study analyzes the 3D movements data and electromyographic signal data. In this part, the 3D movements data and electromyographic signal data are analyzed to investigate the changes of joint angles and angular velocities in different rope skipping movements, the muscle activation level and the muscle contribution rate in different stages. In the third part, the conclusions of the study are obtained.

2. Methods and materials

2.1. Research objects and instruments

The study was conducted to analyze the single shake jump (jumping up once, the rope body leaps forward over the head and through the feet around the body for one week at 360°) and double shake jump (jumping up once, the rope body leaps forward over the head through the feet around the body for two weeks at 720°) in competitive rope skipping [15]. A total of 60 healthy adults were selected for the study, with the number of males and females being 30, of which 30 were in the experimental and 30 in the control group, with the number of males and females in each group equally distributed. In the experimental group, the candidates were those who had trained for more than three years, with continuous single shake jumps greater than or equal to 180 beats per minute and continuous double shaking jumps greater than or equal to 120 beats per minute. Moreover, they were ranked in all levels of rope skipping competitions. The experimental group candidates needed to be able to skillfully perform the basic movements of single shake and double shake jumping, and the rope skipping process was smooth and standardized. The control group candidates had a

rope skipping time between 0.5–2 years, had not participated in formal rope skipping competitions, and had a continuous single shake jump count of more than 100 times/min and a continuous double shaking jump count of more than 60 times/min. The control group needed to master the basic single shake jump and double shake jump action essentials, and was able to stably complete the whole rope skipping process, basically without errors. The average age of the experimental group was 22.14 ± 2.17 years old, the average height was 175.26 ± 3.16 cm, the average weight was 67.03 ± 10.14 kg, and the rope skipping training time was 4.15 ± 0.27 years. The average age of the control group was 23.36 ± 1.59 years, the average height was 176.08 ± 2.94 cm, the average weight was 66.18 ± 9.65 kg, and the rope skipping training time was 1.27 ± 0.18 years. The *P*-values for age, height and weight were all greater than 0.05, and there was no significant difference between the groups. *P*-value for rope skipping training time was less than 0.05 and there was significant difference between the groups.

Inclusion criteria: All subjects had not performed high-intensity exercise within 24 h before the test, and had not suffered any limb or body sports injuries within 1 year, and all joints, such as shoulders, elbows, knees, and ankles, were stable without injuries. Each subject's dominant hand was the same side, no other diseases, before the experiment, they all carried out sufficient warm-up activities, and were able to play their own level stably. Exclusion criteria: An injury or other physical discomfort occurred during the test. The testing apparatus and equipment used in the study are shown in **Table 1**.

Table 1. Specific parameters of test instruments and equipment.

Instrument name	Model number	Manufacturer	Norm
Vicon Three-dimensional motion capture system	T40	Vicon, Britain	Sampling frequency 250 Hz
Electromyograph	Telemyo24000DTS	Noraxon, America	Sampling frequency 1.5 kHz
Kistler ergograph	9260AA6	Kistler, Switzerland	Sampling frequency 1.5 kHz
Loop double touch handle	U1	LOOP, China	Rope length 3 m, diameter 2.5 mm
Laptop	Y7000	Lenovo, China	i7-13650HX, 4060

In **Table 1**, the electromyographic signal tester also includes an acquisition master, 16-channel wireless electromyographic module, and synchronized acquisition box. The 3D movements capture system also includes an infrared shooting head, a calibration frame, and multiple optical localization points. The force platform consists of four 50 cm × 60 cm force plates, support legs, attack legs, four piezoelectric 3D force sensors, and a built-in charge amplifier. Other equipment includes several sensor chargers, several muscle patches, gauze, and sterilized alcohol [16].

2.2. Research method and steps

Before the start of the test, the teste performs an in-situ high leg warm-up activity to move the legs, joints and ligaments and improve flexibility. At the same time, it can ensure that the subsequent test can be completed smoothly and reduce the probability of the tester's injury. The specific experimental steps are shown in **Figure 1**.

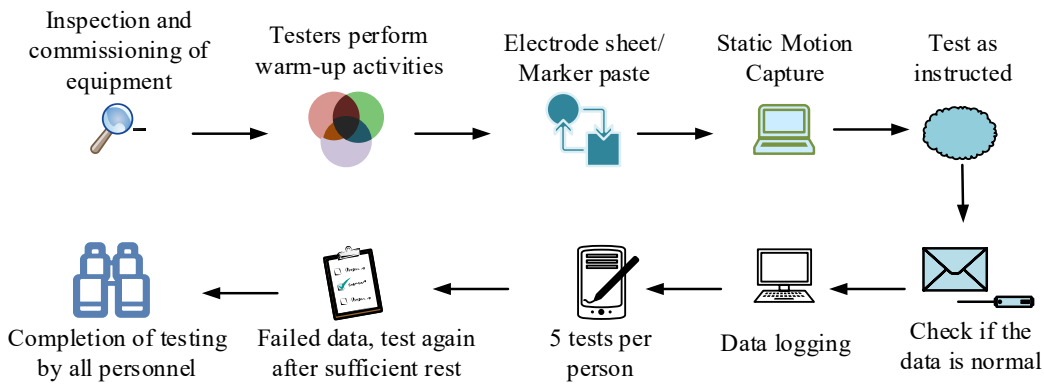

Figure 1. Experimental test procedure.

In **Figure 1**, the related equipment is first checked and debugged. Various experimental supplies are prepared, and the electrode sheets and reflective Marker balls are attached after the tester has finished warming up. The upper body muscles are exposed, and the skin preparation knife is used to scrape off the hair and keratin at the test muscles, and then the electrode sheet is stained to the muscle bulge. The electrodes are then fixed with medical tape to ensure that they do not fall off during the experiment. The reflective sphere can be affixed by directly referring to the model affixing scheme provided by Vicon. After the paste is completed, the acquisition of the tester's static movement is carried out. Subsequently, the test starts according to the instruction, and it needs to be restarted if there is a mistake in the middle of the test [17]. The exact location of the modeled point paste provided by Vicon is shown in **Figure 2**.

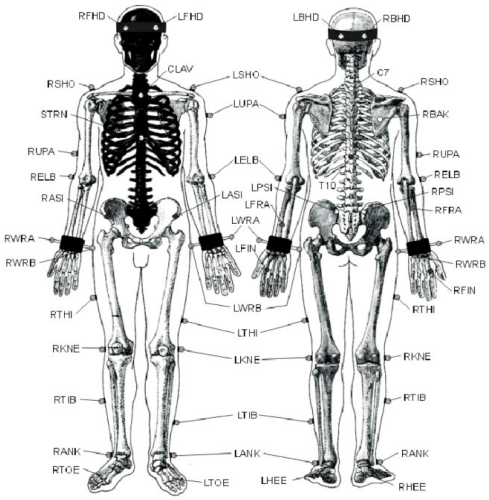

Figure 2. Vicon's modeling point-pasting scheme.

In **Figure 2**, the paste points include 6 points labeled on the head, 5 points labeled on the torso, 6 points labeled on the upper limbs including the right and left shoulders, the right and left elbows as well as the right and left wrists, and 6 points labeled on the lower limbs including the right and left hips, the right and left knees as well as the right and left ankles. In order to improve the accuracy of motion capture, the Vicon system was calibrated before the experiment started by removing all reflective objects in the room to reduce the error. The cameras were calibrated using the calibration bar

provided by Vicon in the calibration window calibrate to calibrate the external parameters between the cameras. When calibrating, you need to wave the calibration rod in the camera area until the sample bars all turn green, then click the calibration button to complete the calibration, and the calibration error needs to be less than 0.3 mm after the calibration is completed. After the test is completed, the relevant data are checked for normalcy and recorded, and each person needs to perform the test five times. The position of the electrode pads affixed for electromyographic signal acquisition is shown in **Table 2**.

Table 2. Test muscle names and electrode paste.

Muscle name	Position	Muscle characteristics	Electrode label	Serial number
Trapezius	Subcutaneous neck and back	Large and flat	TR	1
Deltoid	Lateral shoulder	Provides shoulder flexibility	DE	2
Biceps long head	Tuberositas supraglenoideae scapulae	/	BL	3
Lateral triceps brachii	It begins at the proximal end of the posterior humerus and ends at the olecranon of the ulna	Fiber walking is inclined	LH	4
Flexor carpi radialis	Around the radius and ulna	Medial epicondyle of humerus, deep fascia of forearm	LT	5
Brachioradialis	Most lateral forearm muscle	oblong	BC	6

After the experiments are completed, the electromyographic data are exported using Biometrics analysis software, which includes second-order low-pass filtering, electromyographic envelope maps, rectification-corrected electromyographic signal, and band-pass filtering. The data need to be calculated, in which the integral electromyographic values of the muscles of each part of the limb are calculated as shown in Equation (1) [18].

$$IEMG = \int_{t_1}^{t_2} |X(t)|\, dt \tag{1}$$

In Equation (1), $IEMG$ denotes the integrated electromyographic value. t_1 denotes the integration starting point. t_2 denotes the end point of integration. $X(t)$ denotes the electromyographic signal as a function of time, and the unit of the integrated electromyographic value is mv-s. The RMS amplitude is calculated as shown in Equation (2) [19].

$$RMS = \sqrt{\frac{1}{T}\int_{0}^{T} x^2(t)\, dt} \tag{2}$$

In Equation (2), RMS denotes the RMS amplitude. T denotes the signal period. $x(t)$ denotes the amplitude of the signal at moment t. The contribution of muscles at each location is calculated as shown in Equation (3) [20].

$$C_i = \frac{IEMG_i}{IEMG_z} \times 100\% \tag{3}$$

In Equation (3), C_i denotes muscle contribution rate. $IEMG_i$ denotes the integral electromyographic value of a particular muscle. $IEMG_z$ denotes the sum of the integral electromyographic values of the whole body muscles. The OpenSim model is scaled according to the experimentally measured muscle morphology parameters and related experimental data to establish a personalized model that meets the individual characteristics of the subjects. The specific flow of the OpenSim model is shown in **Figure 3**.

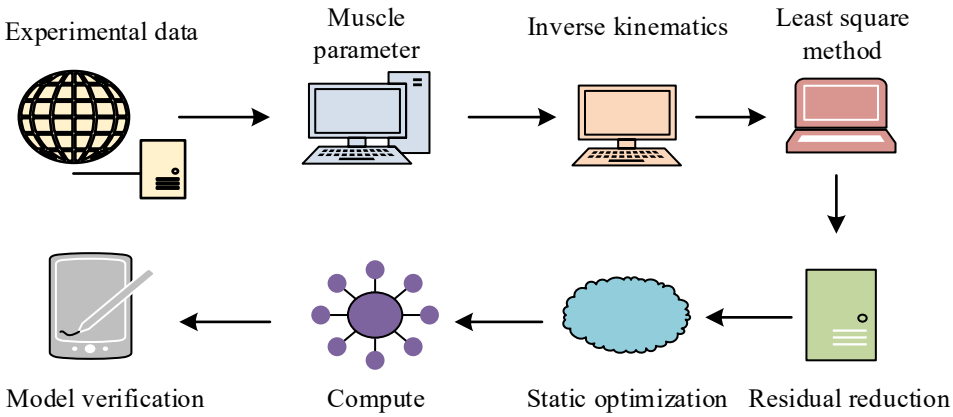

Figure 3. OpenSim model specific flow.

In **Figure 3**, there are usually some errors between the experimental measurements and the actual values of the model when model scaling is performed, so the least squares method is used to calculate the error values. The model and the actual situation of the individual are optimally matched by solving the inverse kinematics. The model combines the external forces with the inertia parameters of the human body through the residual reduction method to minimize the error in the inverse kinematics calculation. The model uses static optimization to decompose the joint moments into a single muscle force at each time. The weighted least squares method is used to calculate the corresponding error values, which are calculated as shown in Equation (4) [21].

$$\min_q \left(\sum_{i \in markers} \omega_i \left(s_i^l - s_i^m \right)^2 + \sum_{j \in coords} \omega_j \left(x_j^l - x_j^m \right) \right) \tag{4}$$

In Equation (4), q denotes the coordinate vector. $markers$ denotes the orientation of the marked point. $coords$ denotes the coordinates of the marked point. ω_i denotes the coordinate weight of point i. ω_j denotes the coordinate weight of point j. s_i^l denotes the measured coordinates of point i. s_i^m denotes the actual coordinates of point i. x_j^l denotes the measured value of point j. x_j^m is the actual value of point j. The residual force in the residual reduction is calculated as shown in Equation (5) [22].

$$F_r = m \cdot a - F \tag{5}$$

In Equation (5), m denotes the mass of the object. a denotes the acceleration. F_r denotes residual force. F is the experimentally measured force.

2.3. Statistical methods

Experimentally measured relevant data were statistically and analytically analyzed using SPSS 22.0, and each test parameter was expressed using x ± s, while all data were tested for conformity to normal distribution. Data that conformed to normal distribution were analyzed using two-factor repeated measures ANOVA, and for some of the data that excluded normality this case has been non-parametric test. The data were analyzed for significance. In this case, $P > 0.05$ indicates that there is no significant difference in the data between groups, and $P < 0.05$ indicates that there is a significant difference in the data between groups.

3. Results

3.1. Kinematic analysis of different rope skipping maneuvers

The study takes the complete completion of single shake or double shake rope skipping maneuver as a time point. The pre-swing stage of the rope skipping maneuver is when the tester makes a move in preparation for jumping. The flight stage is when the tester's feet leave the ground and touch the ground again. The buffering stage is when the tester landed on the ground, and then the body buffered and unloaded until it gradually stabilized. A comparison of the time taken by the experimental group and the control group to complete different maneuvers in different stages is shown in **Table 3**.

Table 3. Comparison of the time required to complete different actions at different stages.

Skipping	Rope skipping action stage	Control group (s)	Experimental group (s)	*P*
Single shake	Average time per session	1.74 ± 0.39	1.93 ± 0.38	0.004
Continuous single shake		1.54 ± 0.42	1.62 ± 0.29	0.096
Single double shake		1.69 ± 0.36	1.83 ± 0.28	0.015
Continuous double shaking		1.25 ± 0.03	1.90 ± 0.06	0.008
Single shake	Pre-swing stage time	0.75 ± 0.23	0.93 ± 0.28	0.003
Continuous single shake		0.80 ± 0.30	0.84 ± 0.35	0.045
Single double shake		0.56 ± 0.19	0.78 ± 0.04	0.012
Continuous double shaking		0.45 ± 0.06	0.82 ± 0.07	0.006
Single shake	Flight phase time	0.46 ± 0.07	0.32 ± 0.05	0.130
Continuous single shake		0.34 ± 0.04	0.32 ± 0.09	0.024
Single double shake		0.62 ± 0.13	0.47 ± 0.08	0.051
Continuous double shaking		0.54 ± 0.03	0.45 ± 0.02	0.068
Single shake	Buffering stage time	0.52 ± 0.21	0.54 ± 0.18	0.046
Continuous single shake		0.37 ± 0.84	0.52 ± 0.59	0.048
Single double shake		0.49 ± 0.32	0.56 ± 0.34	0.009
Continuous double shaking		0.15 ± 0.08	0.64 ± 0.02	0.002

In **Table 3**, the single shake, continuous single, single double shake, continuous double shaking of the control group are 1.74 s, 1.54 s, 1.69 s, and 1.25 s, respectively. The single average time of different ropes of the experimental group is 1.93 s, 1.62 s,

1.83 s, and 1.90 s. The average time of different rope shaking and continuous double shaking is 1.74 s, 1.54 s, 1.69 s and 1.25 s, respectively. The average time of different rope shaking and continuous double shaking in the experimental group is 1.93 s, 1.62 s, 1.83 s, and 1.90 s, respectively. From the experimental situation, the experimental group's rope skipping movements are more standardized and more graceful, so the total time spent is higher. Except for the continuous single shake, there are significant differences among the other three groups. In the pre-swing stage, the experimental group also spent more time, and there is a significant difference between all four sets of data for the experimental and control groups. In the flight stage, the experimental group spends less time than the control group because the pre-swing posture is more correct and more training on rope skipping. Among them, the experimental group spends 0.15 s less time than the control group in single double shake, and there is a significant difference between the data of all groups except single shake. In the buffering stage, the experimental group spends more time than the control group. This is because the buffering action of the experimental group is more in place, which can effectively reduce the wear and tear on the joints and reduce the risk of injury, and there is a significant difference between the data of each group. The changes of wrist and elbow joint angles of different rope skipping movements in the experimental group are shown in **Figure 4**.

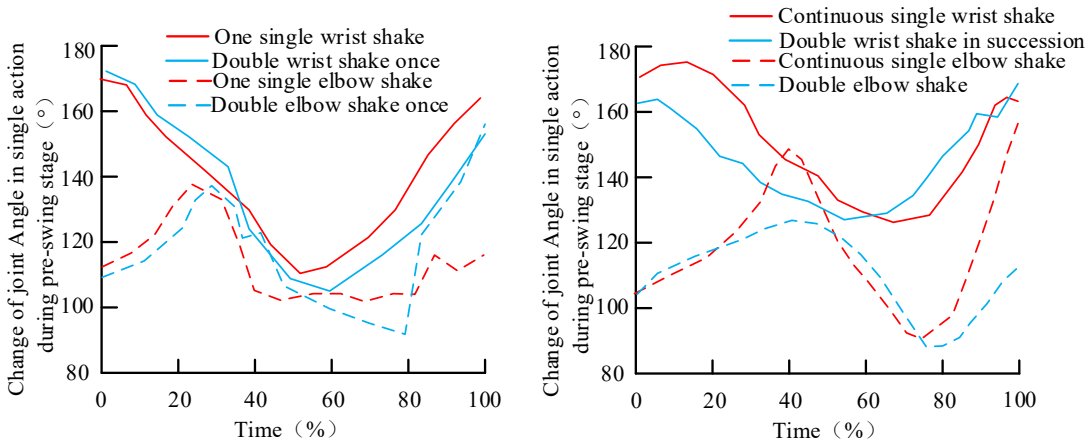

(a) Pre-swing stage single action

(b) Preswing stage continuous action

Figure 4. Comparison of wrist joint and elbow joint angles of different skipping movements in the pre-swing stage.

In the single shake and single double shake of **Figure 4a**, in the pre-swing stage, the average angle of movement of the wrist joint is greater in the single shake than in the double shake, with angle intervals of 116°–168° and 107°–172°, respectively. The average activity angle of the elbow joint is greater for double shake than single shake, and the activity intervals are 104°–138° and 92°–159°, respectively. In **Figure 4b**, both wrist and elbow joints moved more in single rocking than double rocking during continuous rocking of the rope skipping. The maximum angle of activity is 176° at 20% of the duration, the wrist joint is continuous single shake, and the minimum angle of activity is 87°, and the elbow joint is continuous double shaking. A comparison of the wrist joint angular velocity of the experimental group in the pre-swing stage is shown in **Figure 5**.

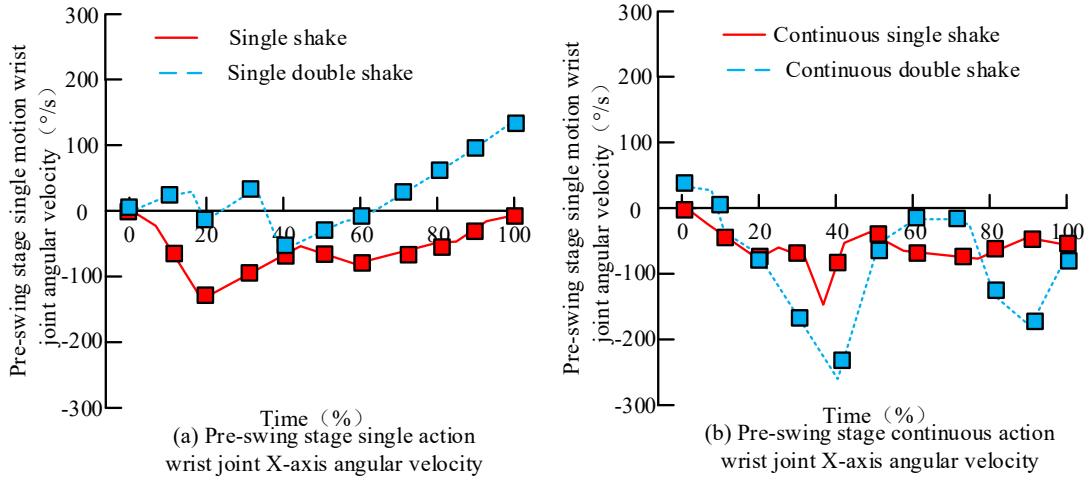

(a) Pre-swing stage single action wrist joint X-axis angular velocity

(b) Pre-swing stage continuous action wrist joint X-axis angular velocity

Figure 5. Comparison of X-axis angular velocity of the wrist joint of the experimental group in the pre-swing stage.

In **Figure 5a**, the angular velocity change of single double shake is much flatter, and the angular velocity of double shake is consistently larger than the angular velocity of single shake. The maximum difference is at 100% of the time, and the difference is 141°/s. The minimum value of the angular velocity of the single shake is at 20% of the time, and the minimum value is 137°/s. The interval of the angular velocity variation of the single double shake is between −67°/s and 148°/s. In **Figure 5b**, the average value of angular velocity of continuous single shake is larger than that of continuous double shake. The angular velocity of single shake is all negative, double shake is positive at time 0%–10%, and the rest is negative. The maximum angular velocity of continuous single shake is 0, and the minimum angular velocity is −253°/s. A comparison of the Y-axis angular velocities of the wrist joint for the pre-swing stage is shown in **Figure 6**.

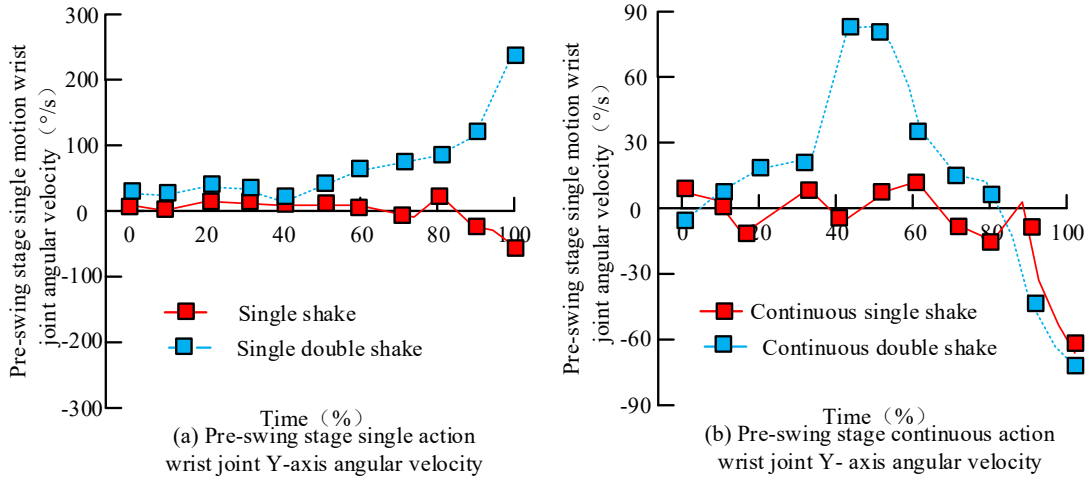

(a) Pre-swing stage single action wrist joint Y-axis angular velocity

(b) Pre-swing stage continuous action wrist joint Y- axis angular velocity

Figure 6. Comparison of Y-axis angular velocity of the wrist joint in the pre-swing stage.

In **Figure 6a**, the wrist joint angular velocity on the Y-axis varies with a gradual increase in single double shake angular velocity, which reaches a maximum value of 235°/s at 100% time. The single shake angular velocity varies in a more zigzag manner, but generally shows a decreasing trend, which achieves a minimum value of 52°/s at 100% time. In **Figure 6b**, the continuous single shake angular velocity varies

zigzaggingly but is generally smaller than the continuous double shaking. The continuous double shaking acceleration peaks at 40% time with a peak value of 88°/s. The minimums are all out at 100% time with −58°/s and −67°/s, respectively. Pre-swing stage lower limb joint angle comparisons are shown in **Figure 7**.

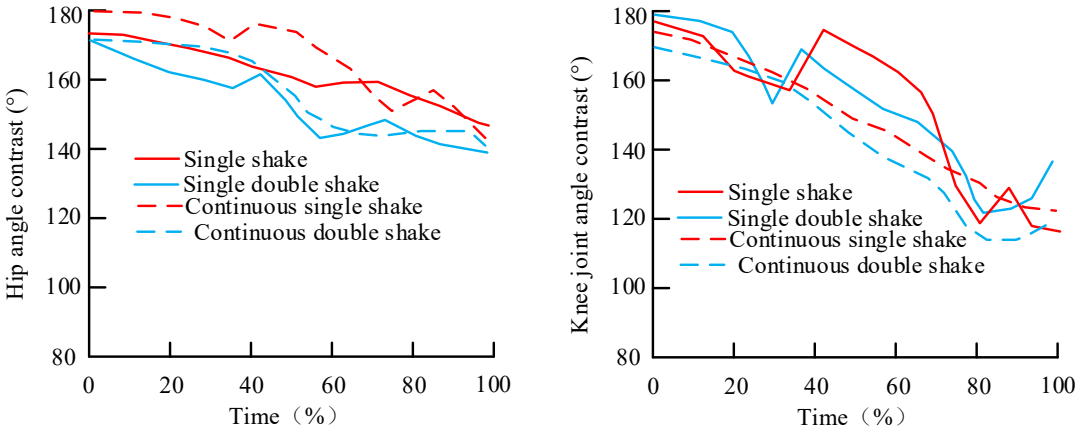

(a) Hip comparison (b) Knee joint comparison

Figure 7. Comparison of lower limb joint angles in pre-swing stage.

In **Figure 7a**, the angle change curves of the hip joints in the lower limbs of the pre-swing stage are in a decreasing trend, and the magnitude of change is approximately the same for the double shake and single shake. The maximum and minimum hip joint angles for single shake are 172° and 158°, respectively, both of which are larger than those for single double shake. The hip joint angle interval of continuous single shake is 179°–154°, and the average angle is larger than that of continuous double shaking. In **Figure 7b**, the angle change curves of the knee joint of the lower limb show an overall decreasing trend, and the curves of the continuous activity are smoother than those of the single activity, with no zigzag points. The interval of knee joint angle for single shake is 178°–124°. The maximum value of knee angle for single double shake is 179° and the minimum value is 131°. The difference between the maximum knee angle for continuous single shake and double shake is small, with minimum values of 128° and 116°, respectively. Comparison of flight stage and buffering stage joint angles are shown in **Figure 8**.

In **Figure 8a**, in the flight stage, the wrist joint angle of single and continuous single shaking is gradually decreasing. Carpal angle for single and continuous double shaking is decreasing, then increasing, then decreasing again. They both have two turning points, both at 20% time and 60% time. The minimum values of the two double shaking wrist joint angles are 127° and 132°, respectively. In **Figure 8b**, in the buffering stage, the knee joint angle is falling and then rising in different movements. The point of rise is at 20% of the time for single shake and at 80% of the time for continuous shake. The minimum values of knee angle for single shake and single double shake are 152° and 128°, respectively. The knee angle minima for continuous single shake and continuous double shake are 121° and 118°, respectively.

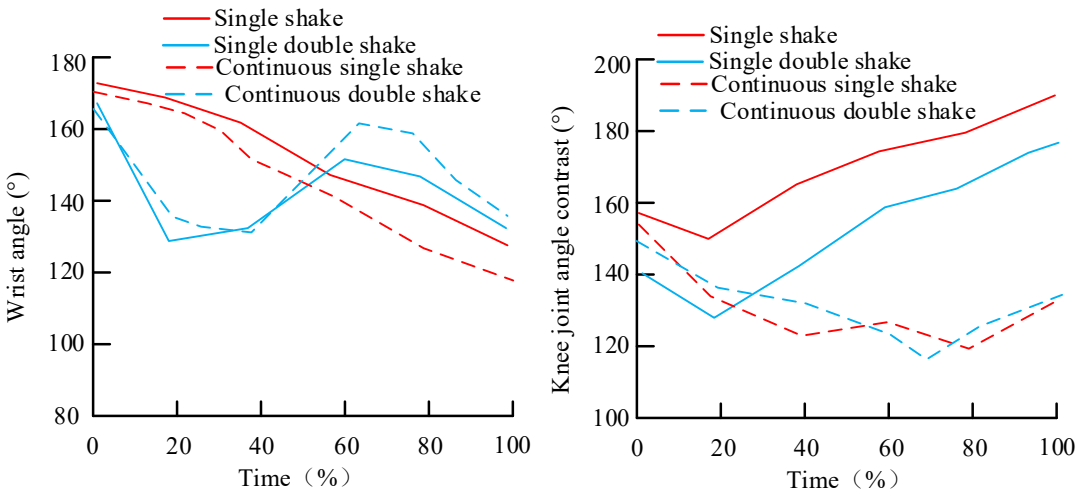

(a) Wrist angle in the flight stage (b) Buffering stage knee angle

Figure 8. Comparison of joint angles between the flight stage and the buffering stage.

3.2. Electromyographic characterization of different rope skipping movements

The study employs different stages of muscle collection level and muscle contribution rate to perform electromyographic characterization of different rope skipping maneuvers. In this case, muscle activation level can be indirectly represented by the RMS amplitude. The muscle contribution rate at each stage is shown in **Table 4**.

Table 4. Muscle activation at each stage.

Muscle	Pre-swing stage				Emptying stage				Buffering stage			
	Single shake	Continuous single shake	Single double shake	Continuous double shaking	Single shake	Continuous single shake	Single double shake	Continuous double shaking	Single shake	Continuous single shake	Single double shake	Continuous double shaking
Trapezius	0.62	0.68	0.44	0.25	0.58	0.63	0.74	0.65	0.29	0.30	0.58	0.61
Deltoid	0.72	0.80	0.33	0.43	0.66	0.72	0.80	0.78	0.55	0.59	0.62	0.63
Biceps long head	0.24	0.31	0.78	0.82	0.60	0.65	0.86	0.88	0.32	0.36	0.30	0.31
Lateral triceps brachii	0.58	0.62	0.49	0.45	0.23	0.18	0.50	0.55	0.52	0.54	0.43	0.42
Flexor carpi radialis	0.32	0.40	0.65	0.77	0.12	0.14	0.35	0.47	0.28	0.53	0.46	0.35
Brachioradialis	0.45	0.52	0.82	0.91	0.76	0.78	0.87	0.89	0.45	0.56	0.39	0.36

In **Table 4**, in the single shake pre-swing stage, the activation of trapezius and deltoid is much higher than the other muscles, with an average of 65% and 66%, respectively. In the double shake pre-swing stage, the activation of biceps long head and brachioradialis is much higher, averaging 80% and 86.5%, respectively. In the flight stage, the activation of all muscles is higher in both single and double swing, except for lateral triceps brachii and flexor carpi radialis. The maximum value is brachioradialis for continuous double shaking with 89% activation. In the buffering stage, the maximum value of muscle activation level for single shake is 28% and the minimum value is 55%. The maximum muscle activation level for continuous

movement is deltoid with an activation level of 59%. The muscle with the highest activation level for both single double shake and continuous double shaking is deltoid with 62% and 63% respectively. The study selected data on the activation level of individual muscles during the failure of some of the rope skipping maneuvers during the experiment. During the single swing pre-swing phase, the activation level of most of the trapezius and deltoid muscles was higher than 70%, with two of the activation levels being less than 50%. At the double-swing pre-swing node, the activation level of the trapezius and deltoid reached 75%, suggesting that the testers may have failed the jump rope maneuver due to higher muscle activation caused by overstressing prior to the start of the jump rope. The muscle contribution rate for each phase is shown in **Table 5**.

Table 5. Comparison of muscle contribution rates in each stage.

Muscle	Pre-swing stage				Emptying stage				Buffering stage			
	Single shake	Continuous single shake	Single double shake	Continuous double shaking	Single shake	Continuous single shake	Single double shake	Continuous double shaking	Single shake	Continuous single shake	Single double shake	Continuous double shaking
Trapezius	21	18	13	7	17	19	18	15	12	12	21	22
Deltoid	23	24	10	12	22	21	18	19	23	21	24	23
Biceps long head	8	11	19	21	18	21	21	19	14	12	11	13
Lateral triceps brachii	19	16	15	11	10	8	12	13	21	20	16	18
Flexor carpi radialis	11	13	15	22	6	6	9	10	11	12	8	8
Brachioradialis	15	15	24	26	25	24	20	19	19	17	16	15

In **Table 5**, in the pre-swing stage, the largest muscle contribution rate in the single shaking maneuver is deltoid. In the double shaking maneuver, brachioradialis has a larger contribution rate. The largest contribution rate is brachioradialis in continuous double shaking at 26%. In the flight stage, all muscles except lateral triceps brachii and flexor carpi radialis have higher contribution in all movements. The brachioradialis contribute the most in all four movements with 25%, 24%, 20%, and 19%, respectively. In the buffering stage, the contribution of each action ranges from 8% to 24%. The largest contribution is deltoid with 23%, 21%, 24%, and 23% for the individual movements.

4. Discussion and conclusion

To investigate the biomechanical characteristics of the athletes when performing different movements in rope skipping, the study employed 3D movements capture and electromyographic signal acquisition to analyze the biomechanics of the athletes during rope skipping. The study could find out the reasonable movement postures and improve the efficiency and quality of movement. The results of the experiment indicated that the total duration of the single maneuver of the experimental group was higher than that of the control group. Except for the flight stage, the time spent on each movement was higher than that of the control group, because the experimental group's rope skipping movements were more standardized, with lower heights in the air and

less cushioning in place, which reduced the risk of injury. In the pre-swing stage, the average movement angle of the wrist joint was greater for single shake than single double shake, and the angle ranges were 116°–168° and 107°–172°, respectively. In the continuous swing, the wrist and elbow joints moved at angles greater for single shake than for double shake. The angular velocity of the double shake was consistently greater than that of the single shake, with a maximum difference of 141°/s at 100% of the time. In flight stage, the wrist angle was gradually decreasing in single and continuous single shake. In the buffering stage, the knee angle decreased and then increased in different movements. The rise points for single and continuous activities were at 20% and 80% of the time, respectively. In the single shake pre-swing stage, the activation of the trapezius and deltoid was much higher than that of the other muscles, 65% and 66%, respectively. In the flight stage, brachioradialis contributed the most. The buffering stage contributed the most to the deltoid, with 23%, 21%, 24%, and 23% for the individual movements, respectively. The study provides personalized injury probability predictions for different sports and individuals by analyzing the changes in joint angles and the level of muscle activation of athletes during exercise, and this personalized analysis can help coaches identify high-risk movements and technical deficiencies in their members so that they can correct faulty movements. The study of the mechanics in sports can help to understand the laws of achieving better performance in sports and to make continuous improvements to effective movements, adjusting training programs to optimize performance. Sports biomechanics analysis can also help to improve relevant sports equipment, including sports shoes and clothing, to further reduce the probability of athletes' injuries. The present study is not without limitations. The muscles selected for electromyographic analysis are located in the upper limbs, which has some implications for the generalizability of the findings. Furthermore, the subsequent electromyographic analysis of the lower limb muscles could be incorporated to enhance the completeness of the biomechanical analysis of rope skipping.

Ethical approval: Not applicable.

Conflict of interest: The author declares no conflict of interest.

References

1. Roupa I, Da Silva M R, Marques F, et al. On the Modeling of Biomechanical Systems for Human Movement Analysis: A Narrative Review[J]. Archives of Computational Methods in Engineering, 2022, 29(7):4915-4958.
2. Ji S, Ghajari M, Mao H, et al. Use of brain biomechanical models for monitoring impact exposure in contact sports[J]. Annals of Biomedical Engineering, 2022, 50(11):1389-1408.
3. Ruiz-Alias S A, Molina-Molina A, Soto-Hermoso V M, et al. A systematic review of the effect of running shoes on running economy, performance and biomechanics: analysis by brand and model [J]. Sports Biomechanics, 2023, 22(3):388-409.
4. Maldonado D R, Banffy M B, Huang D, et al. An increased allograft width for circumferential labral reconstruction better restores distractive stability of the hip: A cadaveric biomechanical analysis[J]. The American Journal of Sports Medicine, 2022, 50(9):2462-2468.
5. Kumar S, Das R. Championing Olympic Excellence: A Bibliometric Analysis of Biomechanics Impacting Tennis Performance on the World Stage[J]. Physical Education Theory and Methodology, 2024, 24(3):494-503.
6. Pleša J, Kozinc Ž, Šarabon N. A brief review of selected biomechanical variables for sport performance monitoring and training optimization[J]. Applied Mechanics, 2022, 3(1):144-159.

7. Harper D J, McBurnie A J, Santos T D, et al. Biomechanical and neuromuscular performance requirements of horizontal deceleration: A review with implications for random intermittent multi-directional sports[J]. Sports Medicine, 2022, 52(10):2321-2354.
8. Peng, X., & Tang, L. Biomechanics analysis of real-time tennis batting images using Internet of Things and deep learning. The Journal of Supercomputing, 2022, 78(4):5883-5902.
9. Tian Y. Biomechanical Properties of Multi-Swing and Single-Swing Rope Skipping Actions[J]. Molecular & Cellular Biomechanics, 2021, 18(1):126-137.
10. Li J, Wu K, Ye D, et al. Effects of Barefoot and Shod Conditions on the Kinematics and Kinetics of the Lower Extremities in Alternating Jump Rope Skipping—A One-Dimensional Statistical Parameter Mapping Study[J]. Bioengineering, 2023, 10(10): 1154-1165.
11. Trasolini N A, Nicholson K F, Mylott J, et al. Biomechanical analysis of the throwing athlete and its impact on return to sport[J]. Arthroscopy, Sports Medicine, and Rehabilitation, 2022, 4(1):e83-e91.
12. Irawan F A, Prastiwi T A S. Biomechanical analysis of the three-point shoot in basketball: shooting performance[J]. Journal of Physical Education and Sport, 2022, 22(12):3003-3008.
13. Li J, Zhang X, Yang G. The Biomechanical Analysis on the Tennis Batting Angle Selection Under Deep Learning[J]. IEEE Access, 2023, 11(5):97758-97768.
14. Gupta R, Dhindsa IS, Agarwal R. Development and Uncertainty Assessment of Low-Cost Portable EMG Acquisition Module. MAPAN, 2024, 39(2):195-209.
15. Barbosa T M, Barbosa A C, Simbaña Escobar D, et al. The role of the biomechanics analyst in swimming training and competition analysis[J]. Sports Biomechanics, 2023, 22(12):1734-1751.
16. Lubis J, Haqiyah A, Kusumawati M, et al. Do problem-based learning and flipped classroom models integrated with Android applications based on biomechanical analysis enhance the learning outcomes of Pencak Silat?[J]. Journal of Physical Education and Sport, 2022, 22(12):3016-3022.
17. Alsaeed R, Hassn Y, Alaboudi W, et al. Biomechanical analytical study of some obstacles affecting the development of football players[J]. International Journal of Physical Education, Sports and Health, 2023, 10(3):342-346.
18. Blanco Ortega A, Isidro Godoy J, Szwedowicz Wasik D S, et al. Biomechanics of the upper limbs: A review in the sports combat ambit highlighting wearable sensors[J]. Sensors, 2022, 22(13):4905-4914.
19. Palmieri-Smith R M, Curran M T, Garcia S A, et al. Factors that predict sagittal plane knee biomechanical symmetry after anterior cruciate ligament reconstruction: a decision tree analysis[J]. Sports Health, 2022, 14(2):167-175.
20. Dornelas RS, Lima DA. Correlation filters in machine learning algorithms to select demographic and individual features for autism spectrum disorder diagnosis[J]. Journal of Data Science and Intelligent Systems, 2023, 3(1):7-9.
21. Hughes G T G, Camomilla V, Vanwanseele B, et al. Novel technology in sports biomechanics: Some words of caution[J]. Sports Biomechanics, 2024, 23(4):393-401.
22. Sedaghat M R, Momeni-Moghaddam H, Heravian J, et al. Detection ability of corneal biomechanical parameters for early diagnosis of ectasia[J]. Eye, 2023, 37(8):1665-1672.